Time-Domain Version of the Physical Theory of Diffraction

Peter M. Johansen

***Abstract*— A time-domain version of the equivalent edge current (EEC) formulation of the physical theory of diffraction is derived. The time-domain EEC's (TD-EEC's) apply to the far-field analysis of diffraction by edges of perfectly conducting three-dimensional (3-D) structures with planar faces illuminated by a time-domain plane wave. By adding the field predicted by the TD-EEC's to the time-domain physical optics (TD-PO) field, a significant improvement is obtained compared to what can be achieved by using TD-PO alone. The TD-EEC's are expressed as the integral of the time-domain fringe wave current (the exact current minus the TD-PO current) on the canonical wedge along truncated incremental strips. Closed-form expressions for the TD-EEC's are obtained in the half-plane case by analytically carrying out the integration along the truncated incremental strip directly in the time domain. In the general wedge case, closed-form expressions for the TD-EEC's are obtained by transforming the corresponding frequency-domain EEC's to the time domain. The TD-EEC's are tested numerically on the triangular cylinder and the results are compared with those obtained using the method of moments in combination with the inverse fast Fourier transform.**

***Index Terms*— Electromagnetic transient scattering, physical theory of diffraction.**

I. Introduction

THE recent advances in the development of short-pulse (broad-band) communication and radar systems have given rise to an increasing interest in the electromagnetic community to formulate time-domain versions of existing frequency-domain techniques for scattering calculations. In particular, time-domain versions of various high-frequency techniques applying to perfectly electrically conducting (PEC) structures with edges have been developed. Among those are the time-domain geometrical theory of diffraction (TD-GTD) and the time-domain uniform theory of diffraction (TD-UTD) for a straight PEC wedge, both derived by Veruttipong [1], and a more general TD-UTD formulation, which also applies to a curved PEC wedge derived by Rousseau and Pathak [2]. Moreover, a time-domain version of the physical optics (TD-PO) approximation has been presented by Sun and Rusch [3] and applied by Sun to the analysis of large reflector antennas [4]. Since the PO approximation is based on radiation from currents it is not subject to the limitation of the ray-optical techniques, namely that they do not apply to configurations for which no isolated stationary points exist on the structure. However, when analyzing structures with edges, the PO approximation usually fails to provide an accurate prediction of the scattered field because it does not (among other things) take into account edge diffraction. In the frequency domain and within the framework of the physical theory of diffraction (PTD) [5], a high-frequency approximation to the edge-diffracted field can be obtained from a line integral along the illuminated part of the edges of the structure by employing one of the closely related approaches known as elementary edge waves [6], incremental length diffraction coefficients [7]–[9], or equivalent edge currents [10]–[13]. A corresponding time-domain version of the PTD can be used to significantly improve the result of what can be obtained using TD-PO alone. However, to the knowledge of the author, such a time-domain version of the PTD has not yet been reported.

The purpose of this paper is to derive a time-domain version of the PTD. This derivation will be based on Michaeli's physical theory of diffraction equivalent edge currents (EEC's) [12]. The time-domain EEC's (TD-EEC's) apply to the far-field analysis of three-dimensional (3-D) PEC structures with planar faces and they take into account the entire first-order edge diffraction and part of the second-order edge diffraction. To enhance the physical insight, the derivation of the TD-EEC's is, whenever possible, carried out directly in the time domain. In this way it clearly appears that the TD-EEC's are based on the time-domain fringe wave (TD-FW) current (the total current minus the TD-PO current) on the canonical wedge and how this current is used to approximate the exact current on 3-D PEC structures.

The paper is organized as follows. In Section II, the TD-FW current on a PEC wedge illuminated by an impulsive plane wave is presented. In Section III, it is explained how the sum of the TD-PO and TD-FW currents on the wedge can be used to approximate the current on 3-D PEC structures with planar faces and straight edges. The far fields radiated by the TD-PO and TD-FW currents on this structure are found in Section IV-A. These far fields, called the TD-PO and TD-FW far fields, respectively, are expressed in terms of traditional surface radiation integrals. To obtain a TD-EEC's formulation, the surface radiation integral representing the TD-FW far field is cast into another double integral in Section IV-B. The outer integral is along the illuminated part of the edges of the structure and the inner integral, representing

Manuscript received September 30, 1997; revised May 26, 1998.

The author is with the Department of Electromagnetic Systems, Technical University of Denmark, DK-2800 Lyngby, Denmark.

Publisher Item Identifier S 0018-926X(99)03732-1.

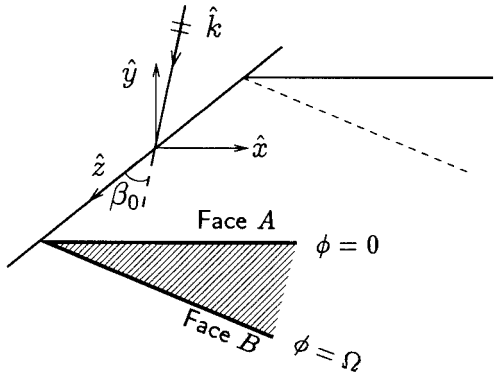

Fig. 1. Three-dimensional view of the PEC wedge under plane-wave illumination.

the TD-EEC's, is along truncated incremental strips on the surface. To obtain closed-form expressions for the TD-EEC's, the inner integral must be calculated analytically. This closed-form analytical calculation is carried out in Section IV-C for the half plane. In the general wedge case, the TD-EEC's are most easily derived by transforming the known FD-EEC's [14], and this is performed in Section IV-D. In Section V, the TD-EEC's are tested numerically on the triangular cylinder. Finally, in Section VI, the general conclusions of the paper are summarized. This paper is a condensed version of [15].

II. The Time-Domain Fringe Wave (TD-FW) Current on the Wedge

Consider the PEC wedge in Fig. 1 with the two faces denoted by A and B, respectively. The wedge is illuminated by an impulsive plane wave and is positioned in a usual rectangular xyz coordinate system with the origin O and with the z axis coinciding with the edge of the wedge. Face A is located in the xz plane and $\hat{y}$ is the outward normal unit vector to this face. The exterior wedge angle is denoted by Ω and it is assumed that $\pi < \Omega \leq 2\pi$. The direction of propagation $\hat{k}$ of the incident plane wave is expressed as $\hat{k} = -\hat{x}\sin\beta_0\cos\phi_0 - \hat{y}\sin\beta_0\sin\phi_0 + \hat{z}\cos\beta_0$ where β_0 is the polar angle and $\phi_0 + \pi$ the azimuthal angle.

The TD-FW current $\vec{K}_\delta^{fw}$ on face A of the wedge under illumination by the impulsive plane wave

$$\vec{E}^i(\vec{r}, t) = \vec{E}_0\delta\left(t - t_d - \frac{\hat{k}\cdot\vec{r}}{c}\right) \tag{1}$$

$$\vec{H}^i(\vec{r}, t) = \vec{H}_0\delta\left(t - t_d - \frac{\hat{k}\cdot\vec{r}}{c}\right) \tag{2}$$

is now presented. In (1) and (2), $\delta(x)$ is the Dirac delta function, $\vec{r}$ the position vector, t the time, $\vec{H}_0 = Z^{-1}\hat{k}\times\vec{E}_0$, $\vec{E}_0$ a real constant vector, Z the intrinsic impedance of the medium, c the speed of light in the medium, and t_d the time for which the wave front of the incident plane wave reaches the origin O. The TD-FW current is derived in [15, Appendix A], [16] using the method of inspection [17], [18, p. 24]. By this method the frequency-domain expression for the FW current is cast into the form of a Laplace integral such that the desired TD-FW current is obtained by inspection. In [15], an alternative derivation of the TD-FW current is carried out using the spectral theory of transients [19]–[21]. The result is

$$\vec{K}_\delta^{fw}(\vec{r}, t) = \frac{-cU(c(t-t_d) - \hat{k}^{fw}\cdot\vec{r})}{\Omega x\,\sin^2\beta_0\,\sinh\beta(t)} \cdot\left(H_{z0}(\hat{x}\,\sin\beta_0 + \hat{z}\,\cos\beta_0\,\cosh\beta(t)) \cdot Q(\phi_0, \beta(t)) - \hat{z}\,\frac{E_{z0}}{Z}\,C(\phi_0, \beta(t))\right) \tag{3}$$

with $H_{z0} = \hat{z}\cdot\vec{H}_0$, $E_{z0} = \hat{z}\cdot\vec{E}_0$,

$$\hat{k}^{fw} = \hat{x}\,\sin\beta_0 + \hat{z}\,\cos\beta_0 \tag{4}$$

$$\cosh\beta(t) = \frac{c(t-t_d) - z\,\cos\beta_0}{x\,\sin\beta_0}, \qquad \beta(t) \geq 0 \tag{5}$$

$$Q(\phi_0, \beta(t)) = K(\phi_0 + \pi, \beta(t)) - K(\phi_0 - \pi, \beta(t)) \tag{6}$$

$$K(\psi, \beta(t)) = \frac{\sin p\psi}{\cosh p\beta(t) - \cos p\psi} \tag{7}$$

$$C(\phi_0, \beta(t)) = L(\phi_0 + \pi, \beta(t)) - L(\phi_0 - \pi, \beta(t)) \tag{8}$$

$$L(\psi, \beta(t)) = \frac{-\sinh p\beta(t)\,\sinh\beta(t)}{\cosh p\beta(t) - \cos p\psi} \tag{9}$$

$U(x)$ being the unit-step function, and $p = \pi/\Omega$. The subscript δ in $\vec{K}_\delta^{fw}$ indicates that the TD-FW current is the impulse response. If the TD-FW current is desired for a time dependence $g(t)$ of the incident plane wave, the convolution

$$\vec{K}^{fw}(\vec{r}, t) = \vec{K}_\delta^{fw}(\vec{r}, t) * g(t) = \int_{-\infty}^{\infty}\vec{K}_\delta^{fw}(\vec{r}, t - t')g(t')\,dt' \tag{10}$$

must be carried out. It is noted that (3) for the TD-FW current is exact for all observation points $\vec{r}$ and for all observation times t. By adding to the TD-PO current $2\hat{y}\times\vec{H}^i(\vec{r}, t)U(\pi - \phi_0)$ the TD-FW current, the total current on face A is obtained. The current on face B can be obtained from the result for face A by substitution of variables [15, p. 20].

III. The Time-Domain Current on 3-D PEC Structures

In this section it is explained how the induced current on a 3-D PEC structure can be approximated using the TD-PO and TD-FW currents on the canonical wedge. The validity of the approximation is also addressed. When the current on the 3-D PEC structure is known, the far field from this current can easily be obtained, as will be shown in Section IV-A.

To simplify the following explanations, a simple 3-D PEC structure is now considered in Fig. 2. The top surface S_{Sq} of this 3-D structure is a square plate with sidelength L and it has four straight edges $E_1, \cdots, E_4$ and four corners $C_1, \cdots, C_4$. The structure is positioned in a global rectangular $x_g y_g z_g$ coordinate system with origin O_g at the center of S_{Sq} and

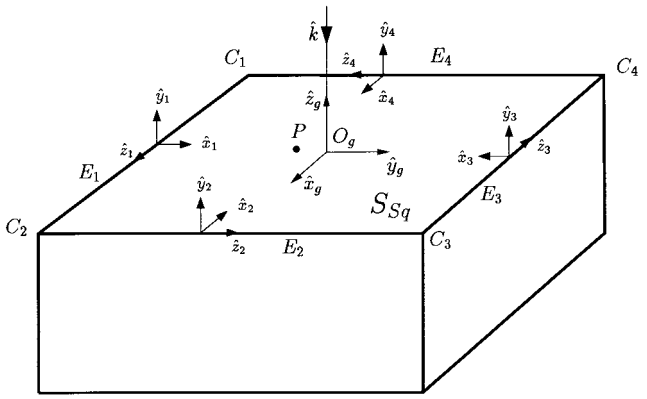

Fig. 2. The simple 3-D PEC structure. The top surface is a square plate with side length L. The current at P described by $-\hat{y}_g y_g$ with $0 < y_g < L/8$ is approximated using four canonical wedges located at the four straight edges $E_1, \cdots, E_4$.

with the x_g axis parallel to E_1 and the y_g axis parallel to E_2. The structure is illuminated by a plane wave described by

$$\vec{E}^i(\vec{r}, t) = \vec{E}_0 g\left(t - \frac{\hat{k} \cdot \vec{r}}{c}\right) \tag{11}$$

$$\vec{H}^i(\vec{r}, t) = \vec{H}_0 g\left(t - \frac{\hat{k} \cdot \vec{r}}{c}\right) \tag{12}$$

where $\vec{E}_0$, $\vec{H}_0$ are defined as in (1) and (2) and the time function $g(t)$ equals zero for $t < 0$. For simplicity, the direction of propagation $\hat{k}$ is chosen to be normal to S_{Sq}, i.e., $\hat{k} = -\hat{z}_g$. The total current $\vec{K}(\vec{r}, t)$ at an observation point P with position vector $\vec{r} = -\hat{y}_g y_g$ where $0 < y_g < L/8$ is desired. This current consists of contributions from several scattering mechanisms. The arrival times of these contributions depend on the direction of propagation $\hat{k}$ and the location of P. With the above choices of $\hat{k}$ and P, the arrival time t^{po} of the PO contribution and the arrival times t^i, $i = C_1, C_2, E_1, \cdots, E_4$, of the contributions from the two corners C_1, C_2, and the four edges satisfy that $t^{po} < t^{E_1} < t^{E_2} < t^{E_3} < t^{C_1}$, $t^{E_4} = t^{E_2}$, and $t^{C_2} = t^{C_1}$. For later observation times there will be contributions from the other corners and from multiple interactions between edges and corners, but these contributions are not of interest for the discussion below.

For $t < t^{E_1}$ the current induced at P on the planar surface S_{Sq} is the same as the current induced on an infinite canonical plane which is tangential to S_{Sq} because the contributions from the edges and corners have not reached P yet. The exact current on this tangent plane is the TD-PO current. Consequently, for $t < t^{E_1}$ the TD-PO current is the *exact* current, i.e., $\vec{K}(\vec{r}, t) = \vec{K}^{po}(\vec{r}, t) = 2\hat{z}_g \times \vec{H}^i(\vec{r}, t)$.[1] The TD-PO current is zero for $t < 0$ because no contributions have reached P yet.

In the interval $t^{E_1} \leq t < t^{C_1}$, the four straight edges $E_1, \cdots, E_4$ contribute to $\vec{K}(\vec{r}, t)$. The contributions from these edges are the same as if each edge had been replaced by the edge of an infinitely long, straight wedge appropriately conforming to the structure because the contributions from the corners have not reached P yet. Hence, for $t < t^{C_1}$ the TD-PO current plus the sum $\vec{K}^{fw,\,tot}(\vec{r}, t)$ of the TD-FW currents excited from the canonical wedges located at the four edges is the *exact* current, i.e., $\vec{K}(\vec{r}, t) = \vec{K}^{po}(\vec{r}, t) + \vec{K}^{fw,\,tot}(\vec{r}, t)$. For the determination of $\vec{K}^{fw,\,tot}(\vec{r}, t)$, a local rectangular $x_i y_i z_i$ coordinate system similar to the one in Section II is introduced at edge E_i, where $i = 1, \cdots, 4$, see Fig. 2. The origin O_i of the $x_i y_i z_i$ system coincides with the stationary point at edge E_i; the first contribution from edge E_i to the current at P stems from this stationary edge point.[2] The sum of the TD-FW currents from the four edges is

$$\vec{K}^{fw,\,tot}(\vec{r}, t) = \sum_{i=1}^{4} \chi_i(\hat{k}, \vec{r}) \vec{K}^{fw,E_i}(\vec{r}, t) \tag{13}$$

where $\chi_i(\hat{k}, \vec{r}) = 1$ if edge E_i is illuminated and simultaneously, a stationary point at that edge exists, and $\chi_i(\hat{k}, \vec{r}) = 0$ otherwise (in this example, $\chi_i = 1$ for all edges). Introducing $\vec{r}_{E_i}$ as the position vector to O_i in the global coordinate system, the contribution $\vec{K}^{fw,\,E_i}$ from E_i is

$$\vec{K}^{fw,\,E_i}(\vec{r}, t) = \vec{K}^{fw}_{\delta}(\vec{r} - \vec{r}_{E_i}, t) * g(t) \tag{14}$$

where $\vec{K}^{fw}_{\delta}(\vec{r} - \vec{r}_{E_i}, t)$ is obtained using the canonical wedge solution (3). The time delay parameter t_d appearing in (3), which is used to account for the fact that the wave front of the incident plane wave arrives at each edge at different times, is $t_d = c^{-1}\hat{k} \cdot \vec{r}_{E_i}$.

For $t \geq t^{C_1}$ the contributions from C_1 and C_2 are present and since these contributions have not been taken into account, the current $\vec{K}(\vec{r}, t)$ can no longer be determined exactly using the canonical wedge. Due to the lack of an exact closed-form solution to the canonical corner problem, the contributions from the corners can only be determined approximately, and not exactly [22].

The fact that the planar surfaces and straight edges of the considered 3-D PEC structure have the same shape as the surface and edge of the canonical wedge is the reason why $\vec{K}(\vec{r}, t)$ can be determined exactly for $t < t^{C_1}$. If the surface is curved, the TD-PO current at an observation point P is not exact even before contributions from edges and corners arrive. However, the TD-PO current is a good approximation to the exact current for early times and this approximation becomes better when the radius of curvature of the surface goes to infinity. The accuracy of the TD-PO current on a curved surface for later observation times is good if most of the energy of $g(t)$ is at sufficiently high frequencies. Similarly, if the structure under consideration has curved edges it is expected that the TD-FW current excited from the straight

[1] If $\hat{k}$ had been chosen so that S_{Sq} is not illuminated then $\vec{K}^{po}(\vec{r}, t) = 0$.

[2] If $\hat{k}$ had been chosen so that E_i is not illuminated or the combination of $\hat{k}$ and P had been chosen so that there is no stationary point at edge E_i, this edge is assumed not to contribute to the current at P. This assumption is the reason for the χ_i-function appearing in (13).

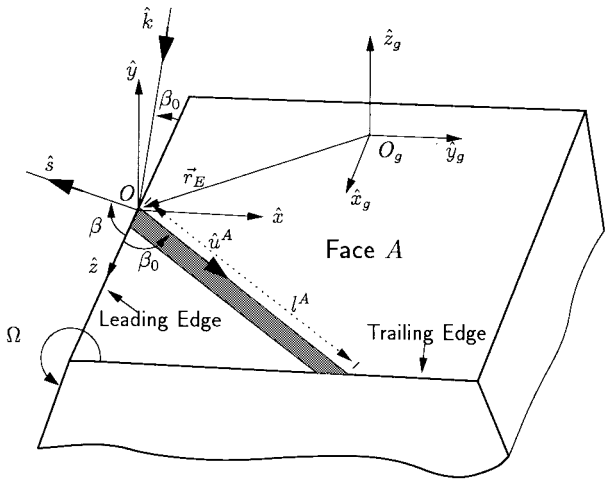

Fig. 3. The truncated incremental strip on face A of the 3-D PEC structure. The direction of the strip is chosen so that the points on the strip have the integration point O as stationary edge point.

canonical wedge becomes a good approximation to the exact current from the curved edge if $g(t)$ has most of the energy at sufficiently high frequencies.

IV. Derivation of the TD-EEC's

In this section, the TD-EEC's are derived. The derivation is performed in three steps. First, in Section IV-A, the TD-PO and TD-FW far fields are expressed in terms of surface radiation integrals of the TD-PO and TD-FW currents found in Section III. Second, the TD-EEC formulation is established in Section IV-B by rewriting the TD-FW surface radiation integral. Third, explicit expressions for the TD-EEC's are obtained in Section IV-C for the half plane and in Section IV-D for the wedge.

A. The TD-PO and TD-FW Far Fields

The configuration under consideration is a more general 3-D PEC structure with planar faces and straight edges than that considered in Section III. The global rectangular $x_g y_g z_g$ coordinate system from Section III is also applied, see Fig. 3, and the incident plane wave is given by (11) and (12). The electric field due to the induced surface current density $\vec{K}$ is at an observation point described by $\vec{s} = s\hat{s}$ in the far-field limit $s \to \infty$ given by [23]

$$\vec{E}(\vec{s}, t) \sim \frac{\vec{\mathcal{F}}\left(\hat{s}, t - \frac{s}{c}\right)}{s} \tag{15}$$

where the far-field pattern $\vec{\mathcal{F}}(\hat{s}, t)$ is

$$\vec{\mathcal{F}}(\hat{s}, t) = \frac{Z}{4\pi c}\,\hat{s} \times \left(\hat{s} \times \int_S \frac{\partial}{\partial t}\vec{K}\left(\vec{r}', t + \frac{\hat{s}\cdot\vec{r}'}{c}\right) dS'\right). \tag{16}$$

Herein, S denotes the surface of the structure and $\vec{r}'$ is the position vector to the integration point.

By substituting $\vec{K}(\vec{r}', t)$ in (16) with the TD-PO current $\vec{K}^{po}(\vec{r}', t)$ [$\vec{K}^{po}(\vec{r}', t) = 2\hat{n}\times\vec{H}^i(\vec{r}', t)$ on illuminated faces, $\hat{n}$ being the outward normal unit vector of the surface, and zero otherwise] the TD-PO far field is obtained. This procedure has been proposed previously by Sun and Rusch [3].

The predicted scattered field can be significantly improved by adding to the TD-PO far field the TD-FW far field which is the field radiated by the TD-FW currents excited from the edges of the structure. A straightforward procedure for obtaining the TD-FW field is to apply the surface radiation integral (16) with $\vec{K}(\vec{r}', t)$ replaced by the sum of the TD-FW currents excited from the N edges found in (13)

$$\vec{\mathcal{F}}^{fw}(\hat{s}, t) = \frac{Z}{4\pi c}\,\hat{s} \times \left(\hat{s} \times \int_S \sum_{i=1}^{N} \chi_i(\hat{k}, \vec{r}')\, \frac{\partial}{\partial t}\vec{K}^{fw, E_i}\left(\vec{r}', t + \frac{\hat{s}\cdot\vec{r}'}{c}\right) dS'\right) \tag{17}$$

where $\vec{K}^{fw, E_i}(\vec{r}', t)$ is defined in (14). Recall that $\chi_i(\hat{k}, \vec{r}') = 1$ if edge E_i is illuminated and simultaneously, a stationary point (with respect to the integration point $\vec{r}'$) at that edge exists and $\chi_i(\hat{k}, \vec{r}') = 0$ otherwise.

According to the discussion in Section III, the TD-PO current at an observation point on a planar surface is exact until edge contributions arrive. Also, the sum of the TD-PO current and the TD-FW currents from straight edges is exact until the corners contribute. However, when considering the far field from structures with planar faces and straight edges illuminated by a plane wave, neither the TD-PO far field nor the sum of the TD-PO and TD-FW far fields is exact at any time. This is due to the fact that edge and corner currents are excited as soon as the plane wave hits the structure. However, the contributions from corners and from multiple interactions between edges and corners are less significant at high frequencies such that the sum of the TD-PO and TD-FW far fields constitutes a good approximation to the exact scattered field if the time function $g(t)$ has most of the energy at sufficiently high frequencies.

Using (17) the first-order edge diffraction is calculated exactly from straight edges.[3] As will be explained after (31), this is not the case for the second-order diffraction. It is observed that for each integration point of the surface radiation integral in (17) one has to find the edges for which a stationary point exists. In the next section, a more efficient procedure, leading to the TD-EEC's, is presented.

B. Rewriting the TD-FW Far-Field Surface Radiation Integral

The basic idea for obtaining a more efficient procedure for calculating the TD-FW far field is the following. Instead of starting with the surface radiation integral in (17), one starts with another double integral which is derived from (17) [10]. The outer integral of this double integral is along the illuminated part Γ of the edges of the structure. For each

[3]The fact that the first-order edge diffraction is calculated exactly does not imply that the first-order diffraction constitutes the exact far field (cf. the previous paragraph).

integration point O of the edge, which in the following will be called the *leading* edge, the inner integral is performed over the TD-FW current excited from that edge along two truncated incremental strips, one on each of the two adjoining faces A and B of the edge, with lengths l^A and l^B, respectively. The truncated strips are terminated at the *trailing* edges, see Fig. 3. The directions of the incremental strips, $\hat{u}^A$ and $\hat{u}^B$, must be chosen so that the points on these incremental strips have O as stationary edge point. Introducing the local xyz coordinate system from Sections II and III with the origin at O, $\hat{x}$ in the plane of face A, $\hat{y}$ normal to face A, and $\hat{z}$ parallel to the edge, the TD-FW far field is

$$\vec{\mathcal{F}}^{fw}(\hat{s},\, t) = \int_{\Gamma} d\vec{\mathcal{F}}^{fw}_{\delta}(\hat{s},\, t) * g(t) \tag{18}$$

with

$$d\vec{\mathcal{F}}^{fw}_{\delta}(\hat{s},\, t) = \frac{Z}{4\pi c}\,\hat{s}\times\left(\hat{s}\times\sum_{i=A,\,B}|\hat{u}^i\times\hat{z}|\int_0^{l^i}\frac{\partial}{\partial t}\vec{K}^{fw}_{\delta}\left(u\hat{u}^i, t+\frac{\hat{s}\cdot(\vec{r}_E+u\hat{u}^i)}{c}\right)du\right)d\Gamma. \tag{19}$$

Herein, $\vec{r}_E$ is the position vector to O in the global system. Using the local system, the unit vector $\hat{s}$ is expressed as $\hat{s} = \hat{x}\sin\beta\cos\phi + \hat{y}\sin\beta\sin\phi + \hat{z}\cos\beta$ where β is the polar angle and ϕ the azimuthal angle. The direction of propagation of the plane wave is $\hat{k} = -\hat{x}\sin\beta_0\cos\phi_0 - \hat{y}\sin\beta_0\sin\phi_0 + \hat{z}\cos\beta_0$ as in Section II. The difference between (17) and (18) is that in (17), the location of the stationary edge points is determined as a function of the integration points on the surface whereas in (18), the integration points on the surface are determined as a function of the location of the stationary edge points.

The calculation of the TD-FW far field would be far less time consuming if the integral along the truncated incremental strips in (19) could be evaluated analytically. It is possible to start with (19) for an analytical evaluation of this inner integral. However, to obtain a time-domain version of the EEC's, (19) is rewritten before an analytical evaluation is initiated. To this end, the incremental TD-FW far field $d\vec{\mathcal{F}}^{fw}_{\delta}$ is expressed in terms of *truncated* equivalent magnetic and electric edge currents, $M_{T,\,\delta}$ and $I_{T,\,\delta}$, as

$$d\vec{\mathcal{F}}^{fw}_{\delta}(\hat{s},\, t) = \frac{1}{4\pi c}\left(Z\hat{s}\times(\hat{s}\times\hat{z})\frac{\partial}{\partial t}I_{T,\,\delta}\left(\vec{r}_E,\, t+\frac{\hat{s}\cdot\vec{r}_E}{c}\right) + \hat{s}\times\hat{z}\,\frac{\partial}{\partial t}M_{T,\,\delta}\left(\vec{r}_E,\, t+\frac{\hat{s}\cdot\vec{r}_E}{c}\right)\right)d\Gamma \tag{20}$$

where $M_{T,\,\delta}$ and $I_{T,\,\delta}$ are the sums of two contributions, one from each of the faces A and B

$$M_{T,\,\delta} = M^A_{T,\,\delta} + M^B_{T,\,\delta} \quad \text{and} \quad I_{T,\,\delta} = I^A_{T,\,\delta} + I^B_{T,\,\delta}. \tag{21}$$

Henceforth, the superscripts A and B refer to the contributions from faces A and B, respectively. In the following, only the contribution from face A will be derived in detail. The contribution from face B is obtained from the result from face A using the substitutions following (31).

The contribution from face A to the truncated TD-EEC's is obtained by equating (19) and (20) [24, eqs. (3)–(7)]

$$M^A_{T,\,\delta} = -Z\sin\beta_0\,\frac{\sin\phi}{\sin\beta}\,L^{A,\,x}_{T,\,\delta} \tag{22}$$

$$I^A_{T,\,\delta} = \sin\beta_0\left(L^{A,\,z}_{T,\,\delta} - \cot\beta\cos\phi L^{A,\,x}_{T,\,\delta}\right) \tag{23}$$

with

$$L^{A,\,x,\,z}_{T,\,\delta} = \int_0^{l^A} K^{fw,\,x,\,z}_{\delta}\left(u\hat{u}^A,\, t+\frac{u\hat{s}\,\cdot\,\hat{u}^A}{c}\right)du. \tag{24}$$

It is important to note that no approximations have been applied to transform (19) into (20). An analytical evaluation of $M^A_{T,\,\delta}$ in (22) and $I^A_{T,\,\delta}$ in (23) makes it possible to calculate $\vec{\mathcal{F}}^{fw}$ simply from a line integral along the illuminated part of the edges of the structure using (18) and (20). The truncated TD-EEC's $M^A_{T,\,\delta}$ and $I^A_{T,\,\delta}$ have no physical meaning. They should be considered as mathematical quantities, which, when integrated using (18) and (20), give exactly the same result as the TD-FW surface radiation integral (17). They represent the integral of the TD-FW current excited from the leading edge along a truncated incremental strip with length l^A.

It is convenient to express the truncated EEC's in terms of the difference between the *untruncated* TD-EEC's and the *correction* TD-EEC's [14]

$$M_{T,\,\delta} = M_{UT,\,\delta} - M_{\mathrm{cor},\,\delta} \quad \text{and} \quad I_{T,\,\delta} = I_{UT,\,\delta} - I_{\mathrm{cor},\,\delta}. \tag{25}$$

The contribution from face A to the untruncated TD-EEC's is

$$M^A_{UT,\,\delta} = -Z\sin\beta_0\,\frac{\sin\phi}{\sin\beta}\,L^{A,\,x}_{UT,\,\delta} \tag{26}$$

$$I^A_{UT,\,\delta} = \sin\beta_0\left(L^{A,\,z}_{UT,\,\delta} - \cot\beta\cos\phi L^{A,\,x}_{UT,\,\delta}\right) \tag{27}$$

with

$$L^{A,\,x,\,z}_{UT,\,\delta} = \int_0^{\infty} K^{fw,\,x,\,z}_{\delta}\left(u\hat{u}^A,\, t+\frac{u\hat{s}\,\cdot\,\hat{u}^A}{c}\right)du. \tag{28}$$

The contribution from face A to the correction TD-EEC's is

$$M^A_{\mathrm{cor},\,\delta} = -Z\sin\beta_0\,\frac{\sin\phi}{\sin\beta}\,L^{A,\,x}_{\mathrm{cor},\,\delta} \tag{29}$$

$$I^A_{\mathrm{cor},\,\delta} = \sin\beta_0\left(L^{A,\,z}_{\mathrm{cor},\,\delta} - \cot\beta\cos\phi L^{A,\,x}_{\mathrm{cor},\,\delta}\right) \tag{30}$$

with

$$L^{A,\,x,\,z}_{\mathrm{cor},\,\delta} = \int_{l^A}^{\infty} K^{fw,\,x,\,z}_{\delta}\left(u\hat{u}^A,\, t+\frac{u\hat{s}\,\cdot\,\hat{u}^A}{c}\right)du. \tag{31}$$

The contribution from face B is obtained from the expressions for face A by replacing β_0 with $\pi-\beta_0$, β with $\pi-\beta$, ϕ_0 with $\Omega-\phi_0$, ϕ with $\Omega-\phi$, and l^A with l^B. The untruncated TD-EEC's, $M^A_{UT,\,\delta}$ and $I^A_{UT,\,\delta}$, express the integral of the TD-FW current excited from the leading edge along an untruncated incremental strip extending to infinity. Thus, when applying the untruncated TD-EEC's no information of the trailing edge is provided and consequently, only the

first-order edge diffraction is accounted for. The correction TD-EEC's $M^{A}_{\mathrm{cor},\delta}$ and $I^{A}_{\mathrm{cor},\delta}$ express the integral of the TD-FW current along another untruncated strip extending from the point of truncation at the trailing edge to infinity. Hence, the correction TD-EEC's provide information of the trailing edge, and consequently, second-order edge diffraction is introduced. However, due to the abrupt truncation of the TD-FW current at the trailing edge, this second-order edge diffraction is not exact as it is the case for the first-order diffraction.

The desired closed-form expressions for the truncated TD-EEC's can now be obtained by carrying out an analytical calculation of the integrals $L^{A,x,z}_{UT,\delta}$ in (28) and $L^{A,x,z}_{\mathrm{cor},\delta}$ in (31). This analytical calculation is performed in the next section for the half-plane case, i.e., when $\Omega = 2\pi$.

C. The TD-EEC's for the Half Plane

By inserting (3) for the TD-FW current on face A in the expressions for $L^{A,x,z}_{UT,\delta}$ in (28) and $L^{A,x,z}_{\mathrm{cor},\delta}$ in (31), setting $\Omega = 2\pi$, calculating the integrals, and adding the contribution from face B (which in this case coincides with face A) the following result is obtained [15, Appendix C]:

$$\frac{\partial}{\partial t} M_{UT,\delta}(\vec{r}_E, t) = \frac{2ZcH_{z0}\sin\phi\,\delta\left(t - c^{-1}\hat{k}\cdot\vec{r}_E\right)}{\sin\beta\sin\beta_0(\mu+\cos\phi_0)} \cdot \left(\frac{\sqrt{2}\cos\dfrac{\phi_0}{2}}{\sqrt{1-\mu}} - \mathrm{sign}\left(\cos\frac{\phi_0}{2}\right)\right) \tag{32}$$

$$\frac{\partial}{\partial t} I_{UT,\delta}(\vec{r}_E, t) = \frac{2\sqrt{2}cE_{z0}\sin\dfrac{\phi_0}{2}\,\delta\left(t - c^{-1}\hat{k}\cdot\vec{r}_E\right)}{Z\sin^2\beta_0(\mu+\cos\phi_0)} \cdot \left(\sqrt{2}\left|\cos\frac{\phi_0}{2}\right| - \sqrt{1-\mu}\right) + \frac{2cH_{z0}\delta\left(t - c^{-1}\hat{k}\cdot\vec{r}_E\right)}{\sin\beta_0(\mu+\cos\phi_0)} \cdot \left(-\mathrm{sign}\left(\cos\frac{\phi_0}{2}\right)(\cot\beta_0\cos\phi_0 + \cot\beta\cos\phi) + \frac{\sqrt{2}\cos\dfrac{\phi_0}{2}\,(\cot\beta\cos\phi - \mu\cot\beta_0)}{\sqrt{1-\mu}}\right) \tag{33}$$

$$\frac{\partial}{\partial t} M_{\mathrm{cor},\delta}(\vec{r}_E, t) = \frac{2ZcH_{z0}\sin\phi U(t')}{\pi\sin\beta\sin\beta_0(\mu+\cos\phi_0)\sqrt{t'}} \cdot \left(-\mathrm{sign}\left(\cos\frac{\phi_0}{2}\right)\frac{C_1}{C_1^2+t'} + \frac{\sqrt{2}\cos\dfrac{\phi_0}{2}}{\sqrt{1-\mu}}\,\frac{C_2}{C_2^2+t'}\right) \tag{34}$$

$$\frac{\partial}{\partial t} I_{\mathrm{cor},\delta}(\vec{r}_E, t) = \frac{2cE_{z0}\sin\dfrac{\phi_0}{2}\,U(t')}{Z\pi\sin^2\beta_0(\mu+\cos\phi_0)\sqrt{t'}} \cdot \left(2\left|\cos\frac{\phi_0}{2}\right|\frac{C_1}{C_1^2+t'} - \sqrt{2(1-\mu)}\,\frac{C_2}{C_2^2+t'}\right) + \frac{2cH_{z0}U(t')}{\pi\sin\beta_0(\mu+\cos\phi_0)\sqrt{t'}}\left(-\mathrm{sign}\left(\cos\frac{\phi_0}{2}\right) \cdot (\cot\beta_0\cos\phi_0 + \cot\beta\cos\phi)\,\frac{C_1}{C_1^2+t'} + \frac{\sqrt{2}\cos\dfrac{\phi_0}{2}\,(\cot\beta\cos\phi - \mu\cot\beta_0)}{\sqrt{1-\mu}}\,\frac{C_2}{C_2^2+t'}\right). \tag{35}$$

In these expressions, the quantities μ, C_1, C_2, and t' are defined by

$$\mu = \frac{\sin\beta_0\sin\beta\cos\phi + \cos\beta_0(\cos\beta - \cos\beta_0)}{\sin^2\beta_0} \tag{36}$$

$$C_1 = \sqrt{\frac{2l^A}{c}}\,\sin\beta_0\left|\cos\frac{\phi_0}{2}\right| \tag{37}$$

$$C_2 = \sqrt{\frac{l^A(1-\mu)}{c}}\,\sin\beta_0 \tag{38}$$

where $l^A = l^B$, and

$$t' = t - c^{-1}\left(\hat{k}\cdot\vec{r}_E + l^A(1-\mu)\sin^2\beta_0\right). \tag{39}$$

General aspects of these TD-EEC's are discussed following (58).

D. The TD-EEC's for the Wedge

When the exterior wedge angle Ω differs from 2π, the calculation of the integrals $L^{A,x,z}_{UT,\delta}$ in (28) and $L^{A,x,z}_{\mathrm{cor},\delta}$ in (31) directly in the time domain is more complicated than in the half-plane case. Therefore, the TD-EEC's for $\Omega \neq 2\pi$ are most easily derived by transforming the corresponding FD-EEC's to the time domain.[4] These FD-EEC's are derived by Johansen in [14] by integrating the FD-FW current along truncated incremental strips. The untruncated FD-EEC's are calculated exactly in closed form whereas a high-frequency approximation is applied to obtain closed-form expressions for the correction FD-EEC's. When $\Omega \neq 2\pi$, the correction FD-EEC's associated with face A are valid only for $kl^A\sin^2\beta_0 \gg 1$, k being the wave number.

The relation between the frequency domain and the time domain is given by the Fourier transform pair

$$f_\omega = \int_{-\infty}^{\infty} f(t)\,\exp(i\omega t)\,dt \tag{40}$$

$$f(t) = \frac{1}{2\pi}\int_{-\infty}^{\infty} f_\omega\,\exp(-i\omega t)\,d\omega \tag{41}$$

[4]This is the only step in the derivation of the TD-EEC's that is not performed directly in the time domain.

where ω in f_ω indicates a frequency-domain quantity. With the application of this Fourier transform pair the Maxwell equations in the frequency domain assume the same form as those of harmonically oscillating fields with the time factor $\exp(-i\omega t)$. Consequently, the frequency-domain solution to a given problem is, except for the dimension, identical to the solution obtained by assuming harmonically oscillating fields.

The untruncated FD-EEC's are given by [14, eqs. (4) and (5)]

$$M^{A,\omega}_{UT,\delta}(\vec{r}_E) = K_1 \frac{\exp\left(ik\hat{k}\cdot\vec{r}_E\right)}{-i\omega} \tag{42}$$

$$I^{A,\omega}_{UT,\delta}(\vec{r}_E) = K_2 \frac{\exp\left(ik\hat{k}\cdot\vec{r}_E\right)}{-i\omega}. \tag{43}$$

The frequency independent quantities K_1 and K_2 are

$$K_1 = \frac{-2ZcH_{z0}\sin\phi}{\sin\beta\sin\beta_0} \cdot\left(\frac{U(\pi-\phi_0)}{\mu+\cos\phi_0} + \frac{\pi\sin p(\pi-\alpha)}{\Omega\sin\alpha(\cos p(\pi-\alpha)-\cos p\phi_0)}\right) \tag{44}$$

$$K_2 = \frac{-2c\pi}{\Omega\sin\beta_0(\cos p(\pi-\alpha)-\cos p\phi_0)} \cdot\left(\frac{H_{z0}\sin p(\pi-\alpha)}{\sin\alpha}(\cot\beta\cos\phi-\mu\cot\beta_0) - \frac{E_{z0}\sin p\phi_0}{Z\sin\beta_0}\right) - \frac{2cU(\pi-\phi_0)}{\sin\beta_0(\mu+\cos\phi_0)} \cdot\left(H_{z0}(\cot\beta\cos\phi+\cot\beta_0\cos\phi_0) - \frac{E_{z0}\sin\phi_0}{Z\sin\beta_0}\right) + \frac{2c\pi\cot\beta_0 H_{z0}}{\Omega\sin\beta_0} \tag{45}$$

with μ defined in (36), α being the solution to $\mu=\cos\alpha$ determined by

$$\alpha = \left(-i\mathrm{Log}\left(\mu+\sqrt{\mu^2-1}\right)\right)^* \tag{46}$$

where $*$ indicates the complex conjugate $\mathrm{Log}z = \ln|z| + i\mathrm{Arg}z$ and $-\pi < \mathrm{Arg}z \le \pi$. The square root in (46) is defined by

$$\sqrt{\mu^2-1} = \begin{cases} -\left|\sqrt{\mu^2-1}\right|, & \mu<-1 \\ i\left|\sqrt{1-\mu^2}\right|, & -1<\mu<1. \end{cases} \tag{47}$$

Although the complex quantity α appears in the constants K_1 in (44) and K_2 in (45), these two constants can be shown to be real [15, p. 62]. Therefore, the untruncated TD-EEC's can now be derived directly by applying the inverse Fourier transform (41) to the frequency-domain expressions (42) and (43)

$$\frac{\partial}{\partial t} M^A_{UT,\delta}(\vec{r}_E,t) = K_1\delta\left(t-c^{-1}\hat{k}\cdot\vec{r}_E\right) \tag{48}$$

$$\frac{\partial}{\partial t} I^A_{UT,\delta}(\vec{r}_E,t) = K_2\delta\left(t-c^{-1}\hat{k}\cdot\vec{r}_E\right). \tag{49}$$

These are the desired expressions for the untruncated TD-EEC's.

The correction FD-EEC's are given by [14, Eqs. (21)–(22)]

$$M^{A,\omega}_{\mathrm{cor},\delta}(\vec{r}_E) \sim K_3\frac{H_{\delta,\omega}(C_1)}{-i\omega} + K_4\frac{H_{\delta,\omega}(C_2)}{-i\omega} \tag{50}$$

$$I^{A,\omega}_{\mathrm{cor},\delta}(\vec{r}_E) \sim K_5\frac{H_{\delta,\omega}(C_1)}{-i\omega} + K_6\frac{H_{\delta,\omega}(C_2)}{-i\omega} \tag{51}$$

for $kl^A\sin^2\beta_0 \gg 1$ when $\Omega \neq 2\pi$. The frequency independent quantities $K_3,\cdots,K_6$ are

$$K_3 = \frac{-2ZcH_{z0}\sin\phi\,\mathrm{sign}\left(\cos\frac{\phi_0}{2}\right)}{\sin\beta\sin\beta_0(\mu+\cos\phi_0)}$$

$$K_4 = \frac{2ZcH_{z0}\sin\phi}{\sin\beta\sin\beta_0}\left(\frac{\sqrt{1-\mu}}{\sqrt{2}(\mu+\cos\phi_0)\cos\frac{\phi_0}{2}} - \frac{\sqrt{2}\pi\sin p\pi}{\Omega\sqrt{1-\mu}(\cos p\pi-\cos p\phi_0)}\right) \tag{52}$$

$$K_5 = \frac{2c\,\mathrm{sign}\left(\cos\frac{\phi_0}{2}\right)}{\sin\beta_0(\mu+\cos\phi_0)} \cdot\left(\frac{E_{z0}\sin\phi_0}{Z\sin\beta_0} - H_{z0}(\cot\beta_0\cos\phi_0+\cot\beta\cos\phi)\right) \tag{53}$$

$$K_6 = \frac{2c\sqrt{2(1-\mu)}}{\sin\beta_0(\mu+\cos\phi_0)}\left(\frac{-E_{z0}\sin\frac{\phi_0}{2}}{Z\sin\beta_0} + \frac{H_{z0}}{2\cos\frac{\phi_0}{2}}(\cot\beta_0\cos\phi_0+\cot\beta\cos\phi) + \frac{\pi H_{z0}\sin p\pi(\mu+\cos\phi_0)(\cot\beta_0-\cot\beta\cos\phi)}{\Omega(\cos p\pi-\cos p\phi_0)(1-\mu)}\right). \tag{54}$$

In (50) and (51), the constants C_1, C_2 are defined in (37) and (38), respectively, and the frequency dependent function $H_{\delta,\omega}$ is

$$H_{\delta,\omega}(C) = \frac{\exp\left(-i\frac{\pi}{4}\right)}{\pi}\exp\left(i\omega\left(c^{-1}\left(\hat{k}\cdot\vec{r}_E + l^A(1-\mu)\sin^2\beta_0\right)-C^2\right)\right)\int_{C\sqrt{\omega}}^{\infty}\exp(it^2)\,dt. \tag{55}$$

The calculation of the correction TD-EEC's requires the transformation of $H_{\delta,\omega}$ in (55) (which involves the Fresnel integral) to the time domain. The transformation is most easily carried out by applying the inverse analytic Fourier transform and this is performed in [2, Appendix] yielding

$$H_\delta(C,t) = \frac{CU(t')}{2\pi\sqrt{t'}(C^2+t')} \tag{56}$$

where t' is defined in (39). It is now a simple task to obtain the correction TD-EEC's from (50) and (51)

$$\frac{\partial}{\partial t} M^A_{\mathrm{cor},\delta}(\vec{r}_E, t) \sim K_3 H_\delta(C_1, t) + K_4 H_\delta(C_2, t) \quad (57)$$

$$\frac{\partial}{\partial t} I^A_{\mathrm{cor},\delta}(\vec{r}_E, t) \sim K_5 H_\delta(C_1, t) + K_6 H_\delta(C_2, t). \quad (58)$$

Since these correction TD-EEC's are obtained by Fourier transforming a high-frequency expression to the time domain, the correction TD-EEC's are most accurate for early times [25], i.e., for $t' \to 0^+$.

This completes the derivation of the untruncated TD-EEC's and the correction TD-EEC's for face A. The contribution from face B is obtained from the results for face A in (48), (49), (57), and (58) using the substitutions following (31). The truncated TD-EEC's, obtained from (25), are then integrated along the illuminated part Γ of the edge using (18) and (20) to obtain the TD-FW far field. Finally, this TD-FW far field is added to the TD-PO far field to yield an approximation to the exact scattered field.

Note that the time dependence of the untruncated TD-EEC's is given by the delta function and consequently, the convolution with an arbitrary time function $g(t)$ is easily performed. By combining the above equations with the expression for $d\vec{\mathcal{F}}^{fw}_{\delta}$ in (20) it is seen that the untruncated TD-EEC's at the integration point on the edge with position vector $\vec{r}_E$ start to contribute to the far field at time $t_1 = c^{-1}\vec{r}_E \cdot (\hat{k} - \hat{s})$. The correction TD-EEC's start to contribute to the far field at time $t_2 = t_1 + c^{-1} l^A (1-\mu)\sin^2\beta_0$. Since the untruncated TD-EEC's account exactly for the first-order diffraction from straight edges, the field produced by the TD-EEC's is the exact first-order diffraction in the time period $t_1 \le t < t_2$. For $t \ge t_2$ the approximate correction TD-EEC's contribute and, therefore, the field produced by the TD-EEC's does no longer constitute the exact edge diffraction. When $\mu = 1$—that is, when $\beta = \beta_0$ and simultaneously, $\phi = 0$—then $t_2 = t_1$, that is, the second-order edge diffraction contributes at the same time as the first-order diffraction. Furthermore, when $\mu = 1$ and simultaneously, $\phi_0 = \pi$ the untruncated TD-EEC's have a nonremovable singularity (the Ufimtsev singularity [12]), but this singularity is cancelled by the corresponding singularity of the correction TD-EEC's. Note that the determination of the times t_1 and t_2 for a general structure is more complicated than in the simple case above where only one integration point is considered.

It follows from the discussions in Sections III and IV-A that the TD-PO far field is calculated exactly from planar faces and that the truncated TD-EEC's predict the first-order far-field diffraction exactly from straight edges. It also follows that the truncated TD-EEC's can be applied to structures with curved edges, but in this case, the first-order diffraction is no longer calculated exactly. However, the approximation of the TD-EEC's to the exact first-order diffraction is expected to become better if the time function $g(t)$ of the plane wave contains sufficiently high frequencies. In addition, since the contributions to the far field from corners and multiple interactions between edges and corners in general becomes less significant for high frequencies, the sum of the TD-PO and the TD-FW far fields becomes a better approximation to the exact scattered far field if $g(t)$ has most of the energy at sufficiently high frequencies.

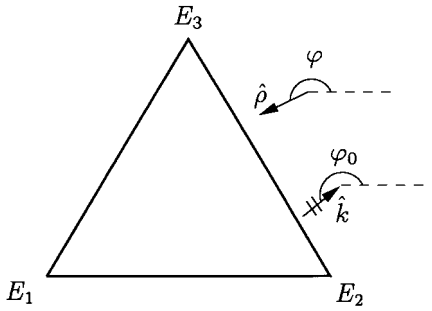

Fig. 4. The triangular cylinder with edges E_1, E_2, E_3. The origin of the coordinate system used in the far-field calculation coincides with edge E_1. The directions of incidence and observation are given by $\varphi_0 = 239^\circ$ and $\varphi = 200^\circ$, respectively.

Through a straightforward calculation it can be shown that the above expressions for the truncated TD-EEC's for $\Omega = 2\pi$ reduce to the half-plane result of Section IV-C, which was derived directly in the time domain. Note that for $\Omega = 2\pi$ the correction TD-EEC's are valid for all observation times, and not only for early times. It should be born in mind, however, that the correction TD-EEC's do still not account exactly for the second-order edge diffraction due to the neglection of the current excited at the trailing edge.

V. Numerical Example

In this section, the truncated TD-EEC's are verified numerically for the infinitely long, triangular cylinder shown in Fig. 4. Although the TD-EEC's are derived to analyze 3-D structures it is convenient to consider this 2-D structure for a first numerical verification. The reason is that the triangular cylinder contains no corners and, thus, the sum of the TD-PO and TD-FW far fields can be exact for a relatively long period of time.

The incident plane wave is impinging upon the structure from the direction given by $\varphi_0 = 239^\circ$ and the time dependence of the plane wave is Gaussian, i.e., $g(t) = \exp(-((ct-1)/0.3)^2)$ in (11) and (12). Both TM and TE polarization (with respect to the cylinder axis) of the incident plane wave is considered. The far-field pattern $\vec{\mathcal{F}}$—defined by $\vec{E}(\vec{\rho}, t) \sim \vec{\mathcal{F}}(\hat{\rho}, t - \rho/c)/\sqrt{\rho}$ as $\rho \to \infty$, $\vec{\rho} = \rho\hat{\rho}$ describing the far-field observation point—normalized with respect to $|\vec{E}_0|$ is now considered in the direction $\varphi = 200^\circ$. This far-field pattern is calculated using both the sum of the TD-PO far field and the field from the truncated TD-EEC's and also the method of moments (MOM) in combination with the inverse fast Fourier transform. The MOM is applied to the FD magnetic field integral equation for TE polarization and to the FD electric field integral equation for TM polarization [26]. A dual-surface formulation has been applied to avoid spurious resonances [27].

Figs. 5 and 6 show the far-field patterns for TE and TM polarization, respectively. In both cases it is seen that the TD-PO far field is very inaccurate because TD-FW currents are excited as soon as the plane wave hits the cylinder. However,

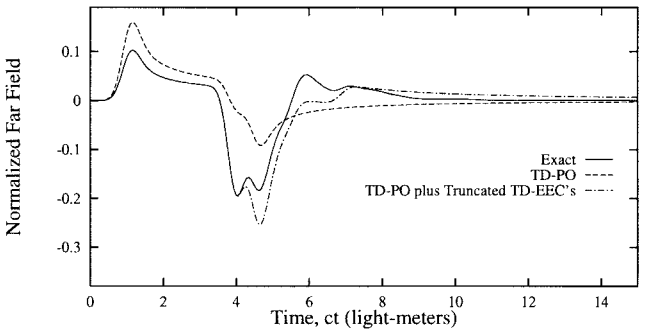

Fig. 5. The far-field pattern for the configuration shown in Fig. 4. The plane wave is TE polarized.

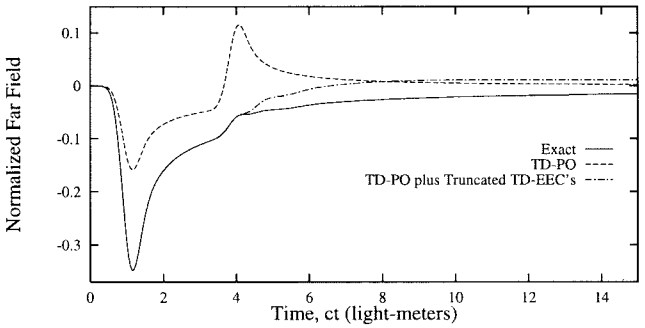

Fig. 6. The far-field pattern for the configuration shown in Fig. 4. The plane wave is TM polarized.

when the field from the truncated TD-EEC's is added, a significant improvement is observed in Figs. 5 and 6. This observation, in combination with the fact that the plane wave has most of its energy at low frequencies, illustrates that the TD-EEC's predict the first-order edge diffraction exactly and not just as an early-time approximation. For large observation times the discrepancy between the MOM solution and the TD-PO plus TD-EEC's solution is caused by two facts. First, the second-order diffraction is not accounted for exactly and second, the diffraction of order higher than two is not included in the TD-EEC's.

VI. Conclusions

TD-EEC's have been derived to analyze the edge diffraction in the far field from 3-D PEC structures with planar faces illuminated by a time-domain plane wave. Using the TD-EEC's, the first-order edge diffraction is calculated exactly from straight edges and approximately from curved edges. The second-order edge diffraction is not calculated exactly for two reasons. First, only part of the second-order diffraction is taken into account due to the neglection of the current excited at the trailing edge. Second, the correction TD-EEC's—which account for the second-order diffraction—are valid only for early times after the arrival of the associated wave front. Although the TD-EEC's account exactly for the first-order diffraction from straight edges, corner contributions will, in general, be present at the same time as the first-order diffraction. Consequently, the sum of the TD-PO far field and the far field from the TD-EEC's constitutes only an approximation to the exact scattered field. This approximation becomes better if the incident plane wave has most of its energy at sufficiently high frequencies.

An interesting future task is the formulation of TD-EEC's for Hertzian dipole illumination of 3-D PEC structures with edges. In this case, the time-domain current on the canonical wedge can also be calculated exactly [28] and the formulation in Section IV-A of the present paper can directly be used to calculate the far field. It would also be interesting to obtain the time-domain analog of a recently formulated PTD method [29], which applies to the analysis of curved PEC surfaces.

Acknowledgment

The author would like to thank Dr. T. B. Hansen for many fruitful discussions on time-domain techniques. He would also like to thank Dr. O. Breinbjerg, Dr. M. Lumholt, and L. S. Andersen for critical comments on the manuscript.

References

[1] T. W. Veruttipong, "Time domain version of the uniform GTD," *IEEE Trans. Antennas Propagat.*, vol. 38, pp. 1757–1764, Nov. 1990.
[2] P. R. Rousseau and P. H. Pathak, "Time-domain uniform geometrical theory of diffraction for a curved wedge," *IEEE Trans. Antennas Propagat.*, vol. 43, pp. 1375–1382, Dec. 1995.
[3] E.-Y. Sun and W. V. T. Rusch, "Time-domain physical-optics," *IEEE Trans. Antennas Propagat.*, vol. 42, pp. 9–15, Jan. 1994.
[4] E.-Y. Sun, "Transient analysis of large paraboloidal reflector antennas," *IEEE Trans. Antennas Propagat.*, vol. 43, pp. 1491–1496, Dec. 1995.
[5] P. Y. Ufimtsev, "Method of edge waves in the physical theory of diffraction," U.S. Air Force, Foreign Technol. Div., Wright-Patterson AFB, OH, 1971 (transl. from Russian).
[6] ———, "Elementary edge waves and the physical theory of diffraction," *Electromagn.*, vol. 11, pp. 125–160, Apr../June 1991.
[7] K. M. Mitzner, "Incremental length diffraction coefficients," Northrop Corp., Tech. Rep. AFAL-TR-73-296, Apr. 1974.
[8] R. A. Shore and A. D. Yaghjian, "Incremental diffraction coefficients for planar surfaces," *IEEE Trans. Antennas Propagat.*, vol. 36, pp. 55–70, Jan. 1988.
[9] ———, "Correction to 'Incremental diffraction coefficients for planar surfaces'," *IEEE Trans. Antennas Propagat.*, vol. 37, p. 1342, Oct. 1989.
[10] A. Michaeli, "Equivalent edge currents for arbitrary aspects of observation," *IEEE Trans. Antennas Propagat.*, vol. AP-32, pp. 252–258, Mar. 1984.
[11] ———, "Correction to 'Equivalent edge currents for arbitrary aspects of observation'," *IEEE Trans. Antennas Propagat.*, vol. AP-33, p. 227, Feb. 1985.
[12] ———, "Elimination of infinities in equivalent edge currents—Part I: Fringe current components," *IEEE Trans. Antennas Propagat.*, vol. AP-34, pp. 912–918, July 1986.
[13] O. Breinbjerg, "Higher order equivalent edge currents for fringe wave radar scattering by perfectly conducting polygonal plates," *IEEE Trans. Antennas Propagat.*, vol. 40, pp. 1543–1554, Dec. 1992.
[14] P. M. Johansen, "Uniform physical theory of diffraction equivalent edge currents for truncated wedge strips," *IEEE Trans. Antennas Propagat.*, vol. 44, pp. 989–995, July 1996.
[15] ———, "Time-domain analysis of electromagnetic scattering problems," Ph.D. thesis, Rep. LD 122, Dept. Electromagn. Syst., Tech. Univ. Denmark, Sept. 1996.
[16] G. Pelosi, G. Manara, A. Freni, and J. M. L. Bernard, "Current evaluation on the faces of an impedance wedge illuminated by an electromagnetic pulse," *IEEE Trans. Antennas Propagat.*, vol. 42, pp. 1663–1667, Dec. 1994.
[17] L. B. Felsen, "Transient solutions for a class of diffraction problems," *Quart. Appl. Math*, vol. 23, pp. 151–169, 1965.
[18] ———, "Propagation and diffraction of transient fields in nondispersive and dispersive media," in *Transient Electromagnetic Fields*, L. B. Felsen, Ed. Berlin, Germany: Springer-Verlag, 1976, ch. 1, pp. 1–72.
[19] E. Heyman and L. B. Felsen, "Weakly dispersive spectral theory of transients—Part I: Formulation and interpretation," *IEEE Trans. Antennas Propagat.*, vol. AP-35, pp. 80–86, Jan. 1987.

[20] _____, "Weakly dispersive spectral theory of transients—Part II: Evaluation of the spectral integral," *IEEE Trans. Antennas Propagat.*, vol. AP-35, pp. 574–580, May 1987.
[21] E. Heyman, "Weakly dispersive spectral theory of transient—Part III: Applications," *IEEE Trans. Antennas Propagat.*, vol. AP-35, pp. 1258–1266, Nov. 1987.
[22] T. B. Hansen, "Corner diffraction coefficients for the quarter plane," *IEEE Trans. Antennas Propagat.*, vol. 39, pp. 976–984, July 1991.
[23] A. D. Yaghjian and T. B. Hansen, "Time-domain far fields," *J. Appl. Phys.*, vol. 79, pp. 2822–2830, Mar. 1996.
[24] A. Michaeli, "Equivalent currents for second-order diffraction by the edges of perfectly conducting polygonal surfaces," *IEEE Trans. Antennas Propagat.*, vol. AP-35, pp. 183–190, Feb. 1987.
[25] S.-W. Lee, V. Jamnejad, and R. Mittra, "An asymptotic series for early time response in transient problems," *IEEE Trans. Antennas Propagat.*, vol. AP-21, pp. 895–899, Nov. 1973.
[26] R. F. Harrington, *Field Computation by Moment Methods.* New York: Macmillan, 1968.
[27] M. B. Woodworth and A. D. Yaghjian, "Derivation, application and conjugate gradient solution of dual-surface integral equations for three-dimensional, multiwavelength perfect conductors," in *PIER 5*, J. A. Kong and T. K. Sarkar, Eds. New York: Elsevier, 1991, ch. 4, pp. 103–129.
[28] L. B. Felsen, "Diffraction of the pulsed field from an arbitrarily oriented electric or magnetic dipole by a perfectly conducting wedge," *SIAM J. Appl. Math.*, vol. 26, pp. 306–312, Mar. 1974.
[29] T. B. Hansen and R. A. Shore, "Incremental length diffraction coefficients for the shadow boundary of a convex cylinder," *IEEE Trans. Antennas Propagat.*, vol. 46, pp. 1458–1466, Oct. 1998.

Peter M. Johansen was born in Roskilde, Denmark, in 1969. He received the M.S.E.E. and and Ph.D. degrees from the Technical University of Denmark, Lyngby, in 1993 and 1996, respectively.

In the spring and summer of 1995, he was a Visiting Research Scientist at the Electromagnetics Directorate of Rome Laboratory, Hanscom Air Force Base, Bedford, MA. In 1997, he was employed by a Danish cellular phone company to work on theoretical aspects of radio wave propagation. In the spring and summer of 1998, he was visiting the Center for Electromagnetics Research at Northeastern University, Boston, MA, while holding a postdoctoral position at the Technical University of Denmark. He is currently an Assistant Research Professor at the Department of Electromagnetic Systems at the Technical University of Denmark. His current research interests include electromagnetic theory, inverse problems, and time-domain scattering.

Dr. Johansen won the first prize of the 1996 IEEE APS Student Paper Contest in Baltimore, MD.